

# Luminescent Vesicles, Tubules, Bowls, and Star Micelles from Ruthenium–Bipyridine Block Copolymers

Kimberly L. Metera and Hanadi Sleiman\*

Department of Chemistry, McGill University, 801 Sherbrooke St. W., Montreal, QC H3A 2K6, Canada

Received October 16, 2006; Revised Manuscript Received February 20, 2007

**ABSTRACT:** We report the first detailed study on the self-assembly of diblock copolymers containing the luminescent metal complex  $\text{Ru}(\text{bpy})_3^{2+}$ , which were constructed by ring-opening metathesis polymerization. Control over the block length, overall polymer length, polymer concentration, and solution conditions has led to the reproducible formation of a number of solution morphologies including vesicles, tubules, large compound micelles, star micelles, and bowls, which all contain  $\text{Ru}(\text{bpy})_3^{2+}$  within the micellar core/vesicle wall. These morphologies hold interesting potential for the facile organization of architectures useful in catalysis and light harvesting.

## Introduction

Ruthenium–bipyridine complexes have been intensely studied in the past three decades due to their interesting and useful photophysical and electrochemical properties. These complexes are relatively stable, absorb in the visible range, and have a large Stokes shift and long luminescence lifetimes. They can also readily undergo electron and energy transfer reactions.<sup>1</sup> As a result of these properties, ruthenium–bipyridine-based complexes have been incorporated into polymers for a number of important applications, such as light-emitting devices, photovoltaic cells, photoconductors, sensors, and light-harvesting devices.<sup>2</sup>

A particularly attractive class of materials are block copolymers containing ruthenium–bipyridine units. Because of their ability to undergo self-assembly into micellar structures, they hold the potential to greatly enhance the range of applications of  $\text{Ru}(\text{bpy})_3^{2+}$  systems. The self-assembly of these block copolymers should result in the confinement of the metal complex within a nanoscale domain of well-defined aggregates. Morphologies such as star micelles or vesicles, for example, can be used to encapsulate reactive molecules for catalysis, segregate electron donors and acceptors to increase the efficiency of solar energy conversion, and to further tune the photophysical properties of the nanoconfined ruthenium centers. However, despite the intense interest in macromolecular systems containing this metal complex, there have been very few methods to construct  $\text{Ru}(\text{bpy})_3^{2+}$  polymers by living polymerization.<sup>2a,3</sup> Polymers incorporating ruthenium–bipyridine units have most often been generated by attaching the complex to a preformed polymer backbone,<sup>4</sup> by nonliving polymerization of a metal-containing monomer,<sup>5</sup> or by using the metal as a junction between different polymer chains in a coordination polymer.<sup>6</sup>

While self-assembly of block copolymers has been extensively investigated, there are far fewer reports on the formation of morphologies from polymers containing transition metals. Ferrocene-containing block copolymers have been investigated in elegant studies by the groups of Manners and Winnik,<sup>7</sup> and a few limited studies on the self-assembly of other block copolymers containing ferrocene,<sup>8</sup> rhenium,<sup>9</sup> cobalt,<sup>10</sup> and palladium<sup>11</sup> have also appeared.

We have previously reported the synthesis of ruthenium–bipyridine-containing polymers and block copolymers by ring-

opening metathesis polymerization.<sup>3</sup> The living nature of this polymerization was established, thus providing ready access to polymers of narrow molecular weight distribution and to the first block copolymers containing a dense arrangement of ruthenium–bipyridine units in one of their blocks. Such polymers possess an unusual architecture and may not self-assemble in solution as predicted on the basis of more commonly investigated polymers. In this report we describe a detailed study of the self-assembly in acetonitrile/toluene mixtures of a series of block copolymers, consisting of a ruthenium–bipyridine-based block and a hydrophobic block. The block length, block ratio, polymer concentration, and solvent composition were systematically varied in order to understand the effects of these parameters on the obtained morphology. We report the observation of a range of morphologies, including star micelles, nanobowls, tubules, and vesicles. In all of these morphologies, the ruthenium complex is confined within the insoluble domain of the aggregate. The predictable formation of the desired morphology in solution is a crucial step in using such self-assembled polymer structures for applications such as catalysis, light harvesting, and sensing.

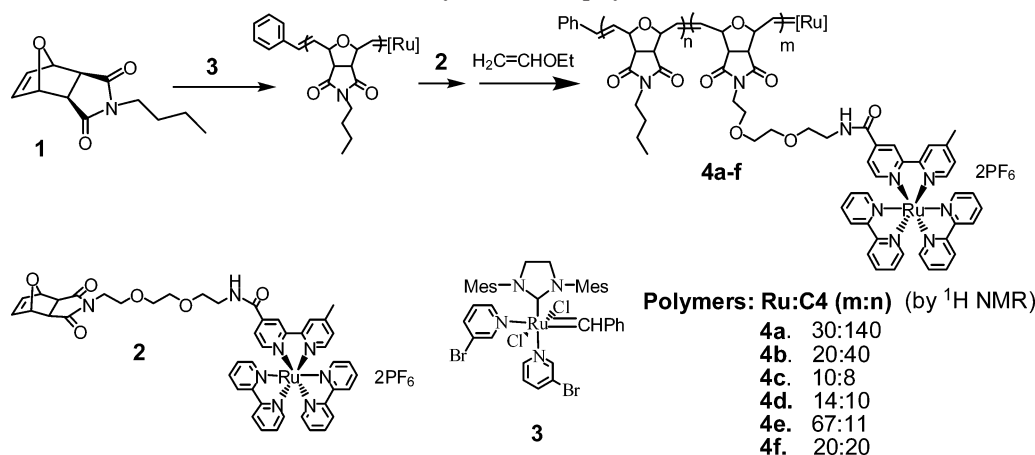
## Results and Discussion

Monomers **1**<sup>12</sup> and **2**<sup>3</sup> and ROMP catalyst **3**<sup>13</sup> were synthesized according to previously published procedures (Scheme 1). Block copolymers **4a–f**, containing a ruthenium–bipyridine block and a hydrophobic block, were generated by sequential addition of monomers **1** and **2** to catalyst **3** in acetone-*d*<sub>6</sub>. In order to systematically study the effect of block copolymer composition on the self-assembly of these molecules, we created a number of such block copolymers **4a–f**, where the ratios of the two blocks as well as the overall polymer length were systematically varied. The polymers were characterized by <sup>1</sup>H NMR, UV/vis, fluorescence spectroscopy, and differential scanning calorimetry (DSC).

We first investigated the generation of simple spherical star micelles from our block copolymers **4**. For this, we synthesized polymers **4a** (Ru:C<sub>4</sub> 30:140) and **4b** (Ru:C<sub>4</sub> 20:40), which possess significantly longer hydrophobic blocks (C<sub>4</sub>) than the metal-containing block (Ru). The two blocks are soluble in acetonitrile, and the hydrophobic block is soluble in toluene, while the ruthenium-containing block is insoluble in this solvent. Upon addition of toluene to an acetonitrile solution of this polymer, aggregation of the copolymer is expected to induce

\* Corresponding author. E-mail: hanadi.sleiman@mcgill.ca.

Scheme 1. Synthesis of Copolymers 4a–f



the formation of morphologies with the ruthenium block in their core and the hydrophobic block as their corona. At high toluene contents, turbidity was observed. Samples were drop-cast onto carbon-coated transmission electron microscopy (TEM) grids. The grids were not stained, since the ruthenium-containing blocks provide sufficient contrast for visualization of the polymers aggregates.

For polymers **4a,b** (initial polymer concentration 5 mg/mL), TEM showed the formation of spherical aggregates at 20% toluene (Figure 1). In addition, as the toluene content of the solution was further increased, no change in morphology was observed for either polymer. Analysis of the TEM images revealed that the micelles formed by both polymer **4a** (Figure 1a) and **4b** (Figure 1b) were approximately 30–40 nm in diameter. This similarity in micellar size was unexpected, considering the large difference in overall length between polymers **4a** (Ru:C<sub>4</sub> 30:140) and **4b** (Ru:C<sub>4</sub> 20:40). However, the lengths of the ruthenium–bipyridine-containing blocks in polymers **4a** and **4b** are estimated to be similar, approximately 16–17 and 11–12 nm, respectively. The observed 30–40 nm diameter is thus likely the result of preferential TEM visualization of the high electron density ruthenium-containing block, rather than the hydrophobic block on the unstained grids. Dynamic light scattering results were more representative of the actual size of these aggregates in solution, showing spherical aggregates for both polymers, with average diameters of about 130 nm for polymer **4a** and 80 nm for polymer **4b**.

Block copolymers containing a larger volume fraction of the insoluble, rather than the soluble block, can fall in the “crew-cut” regime and give rise to a range of morphologies, in addition to micelles.<sup>14</sup> We were interested in exploring the possibility of forming such crew-cut morphologies from copolymers **4**. In the most commonly studied block copolymer systems (e.g.,

polystyrene-*block*-poly(acrylic acid)), the two polymers are usually linear and possess similar structures, and thus a significantly longer insoluble block is required to produce these morphologies.<sup>14</sup> In contrast, the ruthenium-containing, core-forming block in copolymers **4** possesses bulky and positively charged metal complexes with aromatic coordination spheres, attached to the polymer backbone by ethylene glycol-based linkers, and has a high glass transition temperature (Scheme 1,  $T_g = 210\text{ }^\circ\text{C}$  for poly-Ru<sub>19</sub>). The hydrophobic, corona block possesses much smaller and more flexible butyl units. The polymers in this study also contain double bonds along the polymer backbone. Thus, copolymers **4** are not necessarily expected to display parallel structure–morphology relationships to previously reported “crew-cut” polymers.

We first examined the self-assembly of copolymers **4c** (Ru:C<sub>4</sub> 10:8) and **4d** (Ru:C<sub>4</sub> 10:14), which possess a short backbone and similar block lengths, thus a significantly larger volume ratio of the ruthenium-containing block. Using an initial polymer concentration of 25 mg/mL, polymer **4c** showed a range of interesting morphologies upon gradual and slow addition of toluene, such as interconnected bilayer structures (30% toluene, Figure 2a), coexistence of vesicles and interconnected bilayers

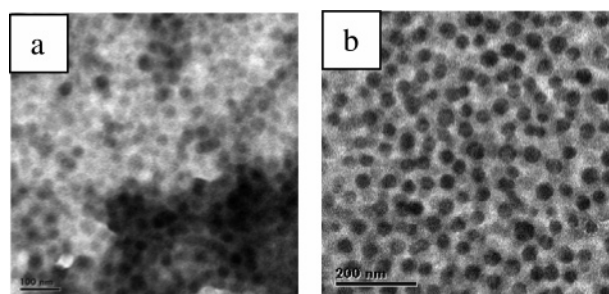


**Figure 1.** TEM images of (a) polymer **4a** and (b) polymer **4b** in 20% toluene in acetonitrile. The scale bar for (a) is 100 nm and 200 nm for (b).

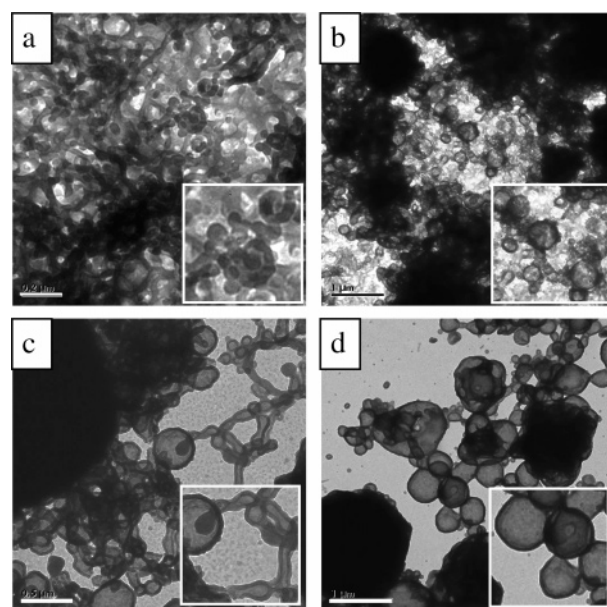


**Figure 2.** TEM images of polymer **4c** as toluene content increases: (a) 30% toluene (scale bar is 200 nm), (b) 40% toluene (1  $\mu\text{m}$ ), (c) 60% toluene (500 nm), (d) 80% toluene (1  $\mu\text{m}$ ). Insets are magnified images.

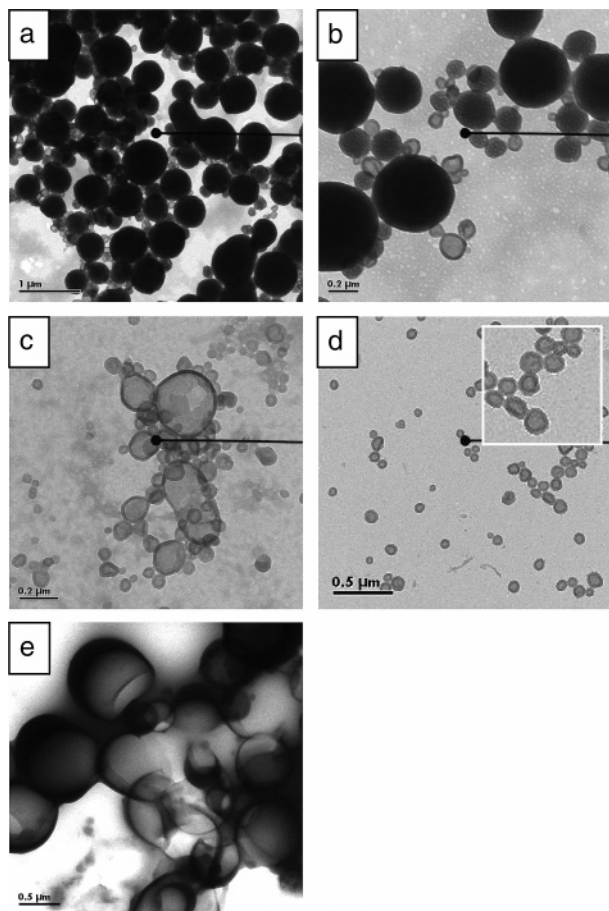


**Figure 3.** TEM images of polymer **4d** as toluene content increases: (a) 40% toluene (scale bar is 1  $\mu\text{m}$ ), (b) 50% toluene (200 nm), (c) 60% toluene (200 nm), (d) 80% toluene (500 nm) (top inset: magnification), (e) bowl structures from polymer **4d** (500 nm).

(40% toluene, Figure 2b), vesicles and tubular structures (60% toluene, Figure 2c), and large spherical bilayers (80% toluene, Figure 2d). The aggregates of polymer **4d** changed even more significantly with toluene content. At initial polymer concentration of 20 mg/mL, the polymer aggregates evolved from predominately large compound micelles (LCM, 40% toluene, Figure 3a), to a coexistence of LCM's and vesicles (50% toluene, Figure 3b), to mainly vesicles with a large size distribution (60% toluene, Figure 3c), to small and uniformly sized vesicles at high toluene contents (80% toluene, Figure 3d). The wall thickness of these vesicles is also uniform at  $\sim 18$  nm (TEM analysis), which is consistent with the length of two ruthenium-containing blocks.<sup>15</sup>

Thus, copolymers **4c** and **4d** show a preference for bilayer morphologies, including luminescent vesicles, tubules, and interconnected bilayers. The formation of stable bilayer morphologies over a range of solvent compositions has been previously reported to occur as a result of the rigidity and stiffness of one of the copolymer blocks.<sup>16</sup> Because of this rigidity, the entropic cost of aggregation is small; thus, the minimization of the interfacial energy dominates the energetics of aggregation, and bilayer structures present smaller interfacial areas than cylinders or spheres.<sup>16</sup> In copolymers **4c** and **4d**, the formation of stable bilayer structures is likely the result of the significant rigidity and high volume ratio of the ruthenium bipyridine-containing block and the presence of the double bonds in the polymer backbone.

Upon more rapid addition of toluene to acetonitrile solutions of polymer **4d**, large compound micelles and, more interestingly,

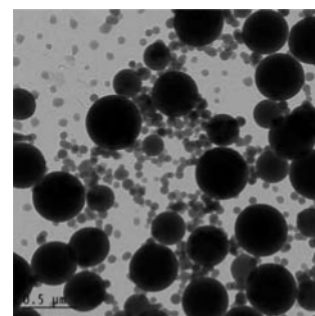


**Figure 4.** TEM image of polymer **4e** in 60% toluene (scale bar is 500 nm).

bowl-like structures were obtained (40–50% toluene, Figure 3e), instead of the previously observed bilayer structures. The sizes of these morphologies were large and polydisperse (200–500 nm, up to 1  $\mu\text{m}$ ). While large compound micelles are relatively common morphologies,<sup>17a</sup> the observation of nanobowl structures from block copolymers has only previously appeared in two recent reports.<sup>17</sup> These intriguing “container” structures are thought to arise in the process of formation of large compound micelles. As the selective solvent (toluene) is added, acetonitrile is drawn out from the spherical aggregates, thus increasing the viscosity and resulting in the formation of a hard “skin” around the sphere, which prevents homogeneous shrinkage. Instead, “polymer-poor” spaces (bubbles) can form, and many of these can coalesce to form a large “bubble”, resulting in a nanobowl morphology.<sup>17</sup> For this to occur, the polymer viscosity should be high enough to cause formation of a “skin” but also low enough to allow coalescence of the bubbles. The ruthenium-containing block most likely endows copolymer **4d** with a high enough viscosity, and the overall short length of both polymer blocks likely places its viscosity within the range required for the generation of bowl morphologies. It is of note that the formation of these nanobowls has been observed reproducibly, using different samples of **4d** and a range of solvent compositions.<sup>18</sup>

Despite the intriguing potential applications of kinetically obtained morphologies such as nanobowls, we were interested in the generation of ruthenium–bipyridine-containing vesicles over a wide range of solvent compositions and conditions and in a method less dependent on the rate of toluene addition. There are exceptionally few accounts of metal-containing polymer vesicles in the literature<sup>19</sup> and none to our knowledge of polymer vesicles with the ruthenium–bipyridine complex as an integral part of the vesicle wall. These structures could allow stable and facile encapsulation of agents for photoinduced electron transfer with the ruthenium complex concentrated in the vesicle wall or the segregation of a donor (e.g., inside the vesicle) and acceptor (e.g., outside the vesicle) using ruthenium–bipyridine as a photomediator. This has exciting potential in applications including sensing, catalysis, and photosynthetic mimicry.

We thus synthesized copolymer **4e**, which possesses a much larger ratio of the insoluble ruthenium-based block (Ru:C<sub>4</sub> 67:11) and is expected to fall more strongly within the “crew-cut” regime. To our knowledge, copolymer **4e** possesses the highest number of ruthenium bipyridine units on a polymer chain reported to date. However, this copolymer (20 mg/mL) only gave rise to the coexistence of large compound micelles with smaller crew-cut micelles, regardless of the toluene content and the rate of toluene addition (Figure 4). The lack of morphological evolution in this copolymer is likely due to the bulkiness of the long ruthenium-containing block and its high glass transition temperature. Initially formed large compound micelle morphol-



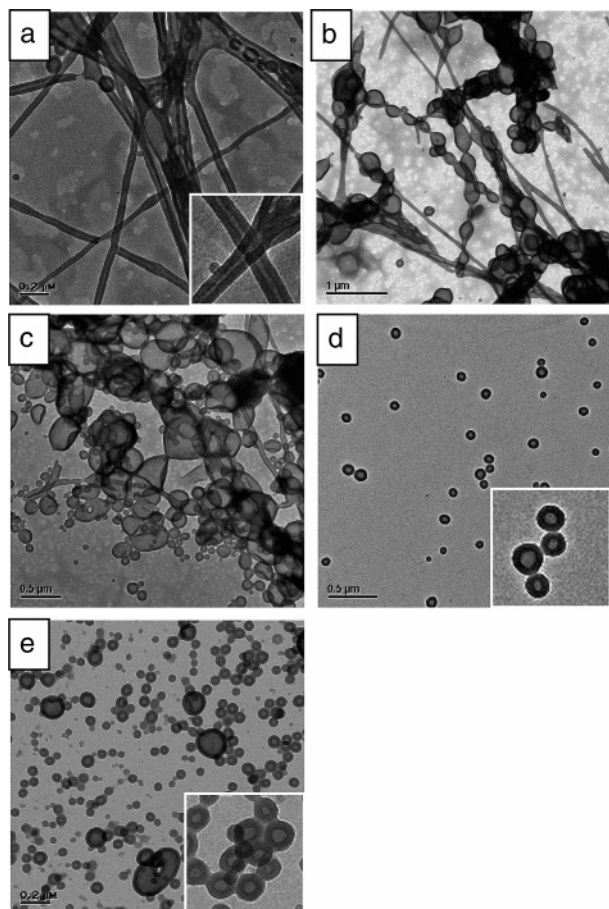


**Figure 5.** TEM images of polymer **4f** as toluene content increases: (a) 20% toluene (scale bar is 200 nm), (b) 35% toluene (1000 nm), (c) 40% toluene (500 nm), (d) 70% toluene (500 nm), (e) polymer **4f** frozen in 70% benzene in acetone (200 nm). Insets are magnified images.

ogies might therefore become kinetically trapped (“frozen”) in solution, and hence these aggregates cannot evolve by the rearrangement of polymer chains as a means of minimizing the energy of the system.

Considering the results obtained with copolymers **4c–e**, we reasoned that kinetically trapped morphologies can possibly be prevented by generating a copolymer with (i) an insoluble metal block that is short enough to allow for rearrangement of polymer chains in solution and (ii) a hydrophobic block that is long enough to solubilize the polymer over a wider range of morphologies than polymers **4c** and **4d**, (iii) but short enough to still place the polymer within the “crew-cut” regime in our solvent system. We therefore synthesized polymer **4f** (Ru:C<sub>4</sub> 20:20), containing a block ratio of 1:1 similar to **4c,d**, but longer than these polymers. Self-assembly of copolymer **4f** in acetonitrile (20 mg/mL polymer)/ toluene solutions of increasing toluene content gave tubule structures (20% and 35% toluene, Figure 5, a and b, respectively) which evolved to large spherical bilayers (40% toluene, Figure 5c), to smaller and more uniformly sized vesicles at higher toluene contents (70% toluene, Figure 5d). The wall thickness of the tubules is approximately 21–22 nm, and that of the vesicles is approximately 26–28 nm; the estimated backbone length of one ruthenium block is approximately 11 nm. These morphologies and their evolution were obtained reliably and reproducibly, and thus kinetically trapped structures were prevented with this polymer.

As mentioned earlier, our TEM imaging method involves evaporation of an acetonitrile/toluene solution of the micellar aggregates of copolymers **4** on a TEM grid. One concern may

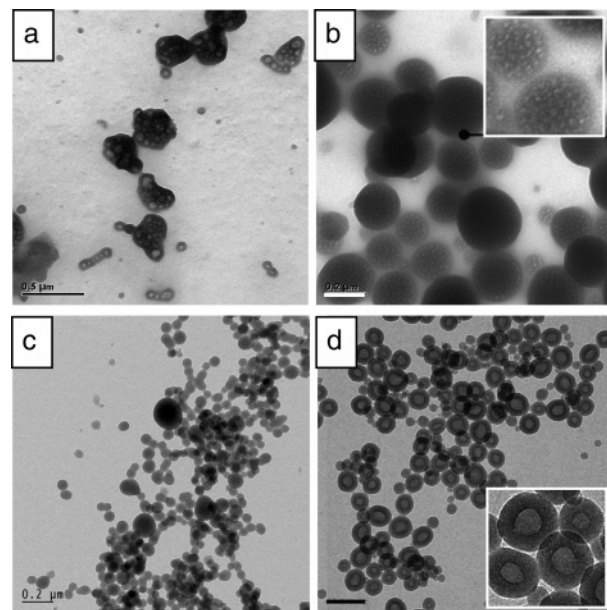


**Figure 6.** TEM images of polymers (a) **4c** (scale bar is 500 nm), (b) **4d** (200 nm), (c) **4e** (200 nm), and (d) **4f** (200 nm) with initial polymer concentration of 5 mg/mL in acetonitrile. Insets are magnified images.

be that this method gives rise to structures which are the result of preferential evaporation of one of the two solvents on the grid and may thus be different from the true solution morphologies. In one attempt to address this, we added toluene to an acetonitrile solution of polymer **4f**, as described above, and removed subsamples not only for drop-casting onto TEM grids as described previously but also for dropping into solutions of pure toluene. This method, in theory, should “freeze” the polymer chains in solution as the instantaneous presence of pure toluene should minimize the rearrangement of polymer chains.<sup>14a</sup> At high toluene concentrations, vesicles were again observed, indicating that these structures are indeed formed in solution.<sup>20</sup> In a second experiment, we prepared TEM samples of **4f** by freeze-drying acetone/benzene solutions of this copolymer, rather than direct room temperature evaporation. (Acetone and benzene were used as an alternative solvent mixture to acetonitrile and toluene, which do not freeze well by this method.) This method is likely to result in TEM images which better reflect the solution morphologies. As shown in Figure 5e, vesicles were also obtained by this preparation from copolymer **4f**. Thus, the preference of copolymer **4f** for vesicle formation is not a result of kinetically trapped structures because of solvent evaporation but is most likely due the presence of these structures on the phase diagram of this copolymer at a range of solvent compositions.

Finally, we examined the self-assembly of copolymers **4c–f** at lower initial polymer concentrations (5 mg/mL). For all polymers, the morphologies observed by TEM did not change significantly as a function of the toluene content in acetonitrile. Polymers **4c** and **4d** appeared to form partially hollow structures (Figure 6, a and b, respectively), and predominantly micelles were obtained for **4e** (Figure 6c). Notably, polymer **4f**, which formed vesicles at high polymer concentrations, also formed vesicles at low concentrations (Figure 6d). The lack of morphology evolution or the apparent kinetic “freezing” of the initially formed aggregates at higher dilution is possibly a result of the low chain mobility of the ruthenium block in these dilute solutions, where the ratio of toluene to this insoluble block is high.

## Conclusion

We have conducted a detailed study of the self-assembly of ruthenium–bipyridine-containing block copolymers, generated by living ring-opening metathesis polymerization. Manipulation of the block ratios, polymer length, and solvent conditions has allowed the reproducible generation of a number of morphologies containing  $\text{Ru}(\text{bpy})_3^{2+}$  units in their micellar core/wall, such as vesicles, star micelles, large compound micelles, tubules, and bowls. These structures, and vesicles in particular, hold exciting potential for the encapsulation and segregation of reactive components and for applications in artificial photosynthesis and catalysis. Work is ongoing to investigate the photophysical properties of these polymers and to explore the encapsulation of reactive species inside vesicles and micelles.

## Experimental Section

**Materials.** Reagents were purchased from Aldrich and used as received. Deuterated solvents were purchased from Cambridge Isotope Laboratories.

**Instrumentation.**  $^1\text{H}$  NMR spectra were recorded on a Varian M400 instrument. Transmission electron microscopy (TEM) images were recorded on a JEOL 2000FX electron microscope operating at 80 kV. 400 mesh carbon-coated grids were purchased from Electron Microscopy Sciences. Dynamic light scattering (DLS) measurements were performed on a Brookhaven Instruments Corp. system equipped with a BI-200SM goniometer, a BI-9000AT digital correlator, and a Compass 315-150 CW laser light source from Coherent Inc. operating at 532 nm (150 mW). Vials were purchased from Canadawide Scientific, and samples were filtered through 0.45  $\mu\text{m}$  PTFE syringe filters from Chromatographic Specialties Inc. Differential scanning calorimetry (DSC) measurements were performed on a TA Instruments model DSC Q1000 instrument calibrated with an indium sample. Polymer samples were heated from 0 to 250  $^\circ\text{C}$  at a rate of 15  $^\circ\text{C}/\text{min}$  under continuous flow of nitrogen of 50 mL/min. Glass transition temperatures were recorded during the second heating scan.

**Synthesis of Copolymers 4.**<sup>3</sup> Monomer **1**<sup>12</sup> and catalyst **3**<sup>13</sup> were mixed in  $d_6$ -acetone, in a sealable NMR tube within a glovebox, and the polymerization was monitored by  $^1\text{H}$  NMR (monomer olefin peaks). When the polymerization was complete, a subsample was removed for quenching, and the ruthenium monomer **2**<sup>3</sup> was added. The reaction was again monitored by  $^1\text{H}$  NMR, and upon completion (2–3 h), the polymerization was quenched with ethyl vinyl ether. The degree of polymerization was determined by NMR: the ratio of the methyl peak of monomer **1** to the terminal phenyl peaks (7.2–7.5 ppm) in the quenched subsample gave the average number of units of monomer **1** per chain, while comparison of the methyl peak of monomer **1** with the bipyridine peaks of the ruthenium-containing block then gave the number of metal units (it is important to note here that we had previously shown that this polymerization under the above conditions is living).<sup>3</sup>

**Self-Assembly.** Polymers **4** were dissolved in acetonitrile at the desired initial concentration, and toluene was added dropwise with  $\sim 5$  s in between drops. At desired intervals a sample of the solution was drop-cast directly onto a TEM grid. Excess solution was wicked away and the grid left to air-dry in a fume hood. For freezing experiments, polymers were dissolved in acetone, and benzene was added dropwise. Two subsamples were removed: one for room temperature deposition onto a grid and the second for deposition onto a grid frozen by placement onto a metal block cooled in liquid nitrogen. The frozen bubble and grid were placed into a vacuum chamber and lyophilized. No TEM sample grids were stained because the ruthenium blocks provide sufficient contrast for visualization.

**Acknowledgment.** This work was supported by NSERC, the Canada Foundation for Innovation, Nanotechnology, Research Corporation, Center for Self-Assembled Chemical Structures,

the Canadian Institute of Advanced Research, and the NSERC Strategic Grant program. The authors thank Dr. Bingzhi Chen for synthesis of polymers **4a** and **4b**. K.L.M. thanks NSERC for a scholarship. H. F. Sleiman is a Cottrell Scholar of the Research Corporation.

**Supporting Information Available:** DLS data for polymers **4a** and **4b** and additional TEM images for polymers **4d** and **4f**. This material is available free of charge via the Internet at <http://pubs.acs.org>.

## References and Notes

- (1) (a) Juris, A.; Balzani, V.; Barigelletti, F.; Campagna, S.; Belser, P.; von Zelewsky, A. *Coord. Chem. Rev.* **1988**, *84*, 85. (b) Kalyanasundaram, K. *Coord. Chem. Rev.* **1982**, *46*, 159–244.
- (2) (a) Carlise, J. R.; Weck, M. J. *Polym. Sci., Part A: Polym. Chem.* **2004**, *42*, 2973–2984. (b) Wu, A.; Yoo, D.; Lee, J.-K.; Rubner, M. F. *J. Am. Chem. Soc.* **1999**, *121*, 4883–4891. (c) Lee, J. K.; Yoo, D.; Rubner, M. F. *Chem. Mater.* **1997**, *9*, 1710–1712. (d) Peng, Z.; Gharavi, A.; Yu, L. *J. Am. Chem. Soc.* **1997**, *119*, 4622–4632. (e) Wang, Q.; Wang, L.; Yu, L. *J. Am. Chem. Soc.* **1998**, *120*, 12860–12868. (f) Wang, Q.; Yu, L. *J. Am. Chem. Soc.* **2000**, *122*, 11806–11811. (g) de Silva, A. P.; Gunaratne, H. Q. N.; Gunlaugsson, T.; Huxley, A. J. M.; McGoy, C. P.; Radem, J. T.; Rice, T. E. *Chem. Rev.* **1997**, *97*, 1515–1566. (h) Beer, P. D. *Acc. Chem. Res.* **1998**, *31*, 71–80. (i) Beer, P. D.; Szemes, F.; Passaniti, P.; Maestri, M. *Inorg. Chem.* **2004**, *43*, 3965–3975. (j) Sykora, M.; Maxwell, K. A.; DeSimone, J. M.; Meyer, T. J. *Proc. Natl. Acad. Sci. U.S.A.* **2000**, *97*, 7687–7691. (k) Chen, M.; Ghiggino, K. P.; Thang, S. H.; Wilson, G. J. *Angew. Chem., Int. Ed.* **2005**, *44*, 4368–4372. (l) Fleming, C. N.; Dupray, L. M.; Papanikolas, J. M.; Meyer, T. J. *J. Phys. Chem. A* **2002**, *106*, 2328–2334. (m) Fleming, C. N.; Maxwell, K. A.; DeSimone, J. M.; Meyer, T. J.; Papanikolas, J. M. *J. Am. Chem. Soc.* **2001**, *123*, 10336–10347. (n) Serin, J.; Schultze, X.; Adronov, A.; Frechet, J. M. J. *Macromolecules* **2002**, *35*, 5396–5404. (o) Dupray, L. M.; Devenney, M.; Striplin, D. R.; Meyer, T. J. *J. Am. Chem. Soc.* **1997**, *119*, 10243–10244. (p) Jones, W. E., Jr.; Baxter, S. M.; Strouse, G. F.; Meyer, T. J. *J. Am. Chem. Soc.* **1993**, *115*, 7363–7373. (q) Fushimi, T.; Oda, A.; Ohkita, H.; Ito, S. *J. Phys. Chem. B* **2004**, *108*, 18897–18902.
- (3) (a) Chen, B.; Sleiman, H. F. *Macromolecules* **2004**, *37*, 5866–5872. (b) Chen, B.; Mettera, K.; Sleiman, H. F. *Macromolecules* **2005**, *38*, 1084–1090.
- (4) (a) Kaneko, M.; Nakamura, H. *Macromolecules* **1987**, *20*, 2265–2267. (b) Marin, V.; Holder, E.; Schubert, U. S. *J. Polym. Sci., Part A: Polym. Chem.* **2004**, *42*, 374–385. (c) Zhou, G.; Harruna, I. I. *Macromolecules* **2004**, *37*, 7132–7139.
- (5) (a) Ito, Y.; Nogawa, M.; Yoshida, R. *Langmuir*, **2003**, *19*, 9577–9579. (b) Holder, E.; Meier, M. A. R.; Marin, V.; Schubert, U. S. *J. Polym. Sci., Part A: Polym. Chem.* **2003**, *41*, 3954–3964.
- (6) (a) Chen, M.; Ghiggino, K. P.; Launikonis, A.; Mau, A. W. H.; Rizzardo, E.; Sasse, W. H. F.; Thang, S. H.; Wilson, G. J. *J. Mater. Chem.* **2003**, *13*, 2696–2700. (b) Johnson, R. M.; Fraser, C. L. *Biomacromolecules* **2004**, *5*, 580–588. (c) Lamba, J. J. S.; Fraser, C. L. *J. Am. Chem. Soc.* **1997**, *119*, 1801–1802. (d) Gohy, J.-F.; Hofmeier, H.; Alexeev, A.; Schubert, U. S. *Macromol. Chem. Phys.* **2003**, *204*, 1524–1530. (e) Gohy, J.-F.; Lohmeijer, B. G. G.; Schubert, U. S. *Chem.—Eur. J.* **2003**, *9*, 3472–3479.
- (7) (a) Massey, J.; Power, K. N.; Manners, I.; Winnik, M. A. *J. Am. Chem. Soc.* **1998**, *120*, 9533–9540. (b) Racz, J.; Manners, I.; Winnik, M. A. *J. Am. Chem. Soc.* **2002**, *124*, 10381–10395. (c) Wang, X.-S.; Winnik, M. A.; Manners, I. *Angew. Chem., Int. Ed.* **2004**, *43*, 3703–3707. (d) Wang, X.; Winnik, M. A.; Manners, I. *Macromolecules* **2005**, *38*, 1928–1935.
- (8) Korczagin, I.; Hempenius, M. A.; Fokkink, R. G.; Cohen Stuart, M. A.; Al-Husseini, M.; Bomans, P. H. H.; Frederik, P. M.; Vancso, G. J. *Macromolecules* **2006**, *39*, 2306–2315.
- (9) (a) Bignozzi, C. A.; Ferri, V.; Scoponi, M. *Macromol. Chem. Phys.* **2003**, *204*, 1851–1862. (b) Hou, S.; Man, K. Y. K.; Chan, W. K. *Langmuir* **2003**, *19*, 2485–2490.
- (10) Miinea, L. A.; Sessions, L. B.; Ericson, K. D.; Glueck, D. S.; Grubbs, R. B. *Macromolecules* **2004**, *37*, 8967–8972.
- (11) Chernyshov, D. M.; Bronstein, L. M.; Borner, H.; Berton, B.; Antonietti, M. *Chem. Mater.* **2000**, *12*, 114–121.
- (12) Bazzi, H. S.; Bouffard, J.; Sleiman, H. F. *Macromolecules* **2003**, *36*, 7899–7902 and references therein.
- (13) Love, J. A.; Morgan, J. P.; Trnka, T. M.; Grubbs, R. H. *Angew. Chem.* **2002**, *114*, 4207–4209.

- (14) (a) Cameron, N. S.; Corbierre, M. K.; Eisenberg, A. *Can. J. Chem.* **1999**, *77*, 1311–1326. (b) Choucair, A.; Eisenberg, A. *Eur. Phys. J. E* **2003**, *10*, 37–44.
- (15) Energy dispersive spectroscopy (EDS) showed the presence of ruthenium, phosphorus, and fluorine in these vesicles. However, the resolution was not sufficient to specifically scan the vesicle wall.
- (16) Antonietti, M.; Forster, S. *Adv. Mater.* **2003**, *15*, 1323–1333.
- (17) (a) Riegel, I. C.; Eisenberg, A. *Langmuir* **2002**, *18*, 3358–3363. (b) Liu, X.; Kim, J.-S.; Wu, Jun.; Eisenberg, A. *Macromolecules* **2005**, *38*, 6749–6751.
- (18) We cannot definitively rule out that these morphologies are a result of the drop-cast sample drying on the TEM grid, although these morphologies have been observed in solution (see ref 17).
- (19) Power-Billard, K. N.; Spontak, R. J.; Manners, I. *Angew. Chem.* **2004**, *116*, 1280–1284.
- (20) We tried several experiments to trap/observe the tubule structures in solution. (i) Dynamic light scattering to detect elongated structures could not be used due to the absorption of the incident laser light and emission from the polymer (a high polymer concentration is necessary for tubule formation). Dilution of solutions of polymer **4f** to perform

DLS measurements resulted in the dissociation of the polymer chains (as confirmed by TEM), likely due to dropping the polymer below its critical micelle concentration. (ii) Freeze-fracture experiments, in which a sample drop is plunged into liquid propane and then sliced and coated with Pt/C to create a replica were also tried. However, removal of the replica from the sample using organic solvent was difficult, and no useful images were obtained. (iii) “Quenching” the tubules by dropping into pure toluene resulted in mainly vesicles by TEM. We believe that when aggregates of polymer **4f** are formed in lower toluene contents (25% toluene) and then dropped into toluene, some rearrangement of polymer chains may occur, possibly due to the small size of the individual polymer chains and the large amount of acetonitrile solvating the ruthenium core; thus, the tubules formed in solution may reorganize into the observed vesicles. (iv) The tubules were, however, obtained reproducibly in many experiments when the solution was drop-cast onto a grid. Such reproducibility might be unexpected if the tubules observed were only a result of drying effects.

MA0623789